Uncertainty Quantification of the Interaction of a Vortex Pair With the Ground

J.L. Sereno[1] **and J.C.F. Pereira**[1]

Abstract: The evolution of a two-dimensional vortex pair in ground effect was studied under the influence of random initial inputs comprising vortex strength (circulation) or initial vortex position. The paper addresses the questions of how do variations and uncertainties of initial conditions translate to the variability of vortex pair evolution. The stochastic solutions were obtained recurring to the Polynomial Chaos Expansion method of random processes applied to the Navier-Stokes equations for a laminar flow. The method quantifies the extent, dependence and propagation of uncertainty through the model system and, in particular, a methodology for the calculation of the vortices trajectory variability, i.e. their confidence interval, could be obtained, provided that the random inputs are not sufficiently high to destroy the mean solutions coherence. The random initial vortex position or the vortex circulation with a variability coefficient of 10% promote after $t^* = 3$, one vortex turnover, vortex trajectories that within a 90% confidence interval display an error bar with lengths up to $2r_0$ (two times the initial vortex radius).

1 Introduction

Most of the engineering problems concerned with solid mechanics or fluid mechanics require the modeling of input or initial uncertainties and their propagation thought the system under consideration, see e.g. Ghanem and Spanos (1991); Cui and Yu (2009); Fleissner and Eberhard (2009); Turrin (2009); Gao (2009). Several stochastic approaches are available nowadays in order to quantify the propagation of uncertainty from the input parameters into the model outputs. Spectral Projection (SP) methods based on Polynomial Chaos (PC) expansion, see e.g. Xiu and Karniadakis (2002); Knio (2006); Najm (2009), are more appropriate and suitable for large degree of parametric uncertainty than the computationally expensive Monte-Carlo (MC) method, see e.g. Caduci (2003) because Monte-Carlo type methods

---

[1] Instituto Superior Técnico, Tech. Univ. Lisbon, LASEF, Lisbon, Portugal.

conduct only statistical analysis on the solution of deterministic simulations performed with randomly selected conditions. The procedure does not readily provide information about the sensitivity of the model output to specific parametric uncertainties. Monte Carlo techniques have a high computational cost due to the required large amount of samples needed, therefore this approach is often restricted to problems with fast deterministic simulations, see e.g. Maître (2001).

PC based methods require the model parameters to be characterized as aleatory uncertainties, i.e. it is presumed that sufficient probabilistic information exists about the parameters Najm (2009). In SP methods, the uncertain model parameters are made dependent on additional random dimensions along with time and space and the stochastic variables of the model are projected on these random dimensions using appropriate PC expansions. The objective of SP methods is to calculate the PC expansion mode coefficients, which are then used to extract probabilistic information about the stochastic model solution, such as statistics, confidence intervals, probability density functions (PDF) or sensitivity to parametric uncertainty.

SP methods may be formulated using two different approaches: intrusive and non-intrusive, see e.g. Cui and Yu (2009); Fleissner and Eberhard (2009). In the Intrusive SP approach, (ISP), the model governing equations are reformulated in order to directly propagate the uncertainty through the model during the simulation, see e.g. Xiu and Karniadakis (2002). Although their approach is effective, it may not be practically suitable for commercial or complex codes. The non-Intrusive SP (NISP) approach evaluates a posteriori the PC expansion mode coefficients of the stochastic model solution using deterministic solution samples. This approach shares with MC methods the advantage of using the original deterministic code as a black box. However as the number of uncertain parameters increases it requires sophisticated methods to implement such that it becomes competitive with the ISP approach (Parussini and Pediroda (2008)). Several authors have compared the two basic strategies embodied in specific numerical methods for fluid flow see Loeven and Bijl (2008); Parussini and Pediroda (2008, 2007).

The objective of this work is to study the stochastic two dimensional interaction of a vortex pair with a wall considering different uncertainty sources: i) Vortex Reynolds number (circulation), ii) Position of the vortices relative to each other. The present study focuses on uncertainties existing in a vortex pair interacting with a wall and the uncertainty quantification problem is addressed using an intrusive spectral projection based method. The study considers relatively low Reynolds number, $Re = 5000$. The same problem at a much higher Reynolds numbers is of direct relevance for aircraft wake vortices. This topic has received particular attention in the past due to their impact in safety and efficiency of airports, see e.g. Spalart (1998); Gerz (2005), for a review.

The physics of wake vortex decay is now well understood but their application to real scenarios faces the problem of large uncertainties in many of the parameters that affect the motion of lift-generated vortex wakes generated by aircrafts. Among the uncertainty parameters the meteorological conditions, wind velocity components (crosswind), turbulence and thermal stratification combined with aircraft weight, type, velocity and distance from the ground, create large uncertainty sources that affect the prediction of the wake-hazardous region for single or parallel runways in busy airports.

The calculation of the stochastic Navier-Stokes equations allows us to capture the events that are more likely to occur and to establish confidence intervals by providing an ensemble of solutions associated to a certain probability of occurrence. The calculation of the stochastic Navier-Stokes equations with classical methods requires a prohibited number of different unsteady Navier-Stokes simulations to obtain converged statistics and a simple parametric study with a smaller number of samples would not be enough to quantify the uncertainty. The present paper investigates the evolution of a vortex pair in ground effect two idealized scenarios. The first scenario comprises the initial circulation is in the range of $0.9\Gamma_0 \leq y \leq 1.1\Gamma_0$ with Γ_0 being the initial vortex circulation. The second scenario corresponds to a vortex pair with the same initial circulation but with the initial vertical position of one vortex is in the range of $0.9y_c \leq y \leq 1.1yc$ with y_c being the initial position of the other vortex.

Stochastic Navier-Stokes simulations allow to answer the following questions: Where is the most probable trajectory? What is the uncertainty (dispersion) along the most probable trajectory? What are the average energy decay and the error bar for a 90% confidence interval? What is the vortex circulation along the most probable trajectory? The present calculations were performed for a Reynolds number of 5000 and up to a non-dimensional time, $t^* = 3$, where the two-dimensionality of the flow structure is supported by three-dimensional numerical simulations by Duponcheel (2006).

2 Stochastic Navier-Stokes Equations

2.1 Governing equations

The important issue of the parameters and the accurate calculation of the propagation of the uncertainty through the model can be performed by the spectral representation of the uncertainty via polynomial chaos (PC). Wiener (1938) proposed a spectral representation of general random variables based on Hermite orthogonal polynomials of the Gaussiam random variable. The span of these orthogonal variables forms a basis for $L2$ and is called a Polynomial Chaos (PC). The PC Ex-

pansion Method for its effectiveness, for short time integration has been used for the calculation of stochastic PDE's (Partial Differential Equations) and is based on the spectral representation of random variables. The PC representation of general random variables is convergent (in the *L2* sense) for the Gaussian measure, provided that the random variable is of second order, see Cameron and Martin (1947). This method was first applied in the context of PDE's with random inputs by Ghanem and Spanos (1991). Later development of decompositions based on non-Gaussian random variables was made by Xiu and Karniadakis (2002) which has been called the Generalized Polynomial Chaos (gPC) and uses orthogonal polynomials from the Askey family with weighting functions similar to PDF's. A formal exposition and a generalization of the theory to arbitrary probability measures were accomplished by Soize and Ghanem (2004). Local PC expansions, suited for long term integration and discontinuities in the stochastic differential equation, were studied by Le Maître, Najm, and Knio (2004). A general random process X of a random variable ξ can be represented using the polynomial chaos expansion

$$X(\xi) = \sum_{n=0}^{\infty} a_n \Psi_n(\xi)$$ (1)

where the functions Ψ_n form a basis of orthogonal polynomials of the random variable in the space *L2* with the inner product

$$\langle u, v \rangle = \int_{\Omega} u(\xi) v(\xi) w(\xi) d\xi$$ (2)

w is the weighting function (defined in Ω) that is similar to a given probability density function (Gaussian, Beta, Binomial,...). Orthogonal polynomials which have weighting functions that closely resemble PDF's can be found in the Askey family of hypergeometric polynomials (Xiu and Karniadakis (2002)). A general differential equation containing random variables can be represented by

$$F(\mathbf{x}, t, \xi, \mathbf{u}) = f(\mathbf{x}, t, \xi)$$ (3)

where x, t and ξ represent the space coordinates, time, and the random variable. Substituting the expansion (1) in the differential equation we obtain the following

$$\left\langle F\left(\mathbf{x}, t, \sum_{n=0}^{P} \mathbf{u}_n \Psi_n\right), \Psi_k \right\rangle = \langle f(\mathbf{x}, t), \Psi_k \rangle$$ (4)

The equation terms can be projected into the space spanned by the polynomial basis in order to absorb the random variable and to minimize the representation error. This procedure leads to (5) and (6) where the first $P+1$ terms were retained. This means that instead of solving a system of differential equations with random variables, one has to solve a larger system of coupled deterministic equations. Assuming the PC-expansions of the primary variables for the Navier-Stokes equations (for an incompressible fluid with constant properties)

$$\mathbf{u}(\mathbf{x},t,\xi) = \sum_{n=0}^{P} \mathbf{u}_n(\mathbf{x},t)\Psi_n(\xi) \tag{5}$$

$$p(\mathbf{x},t,\xi) = \sum_{n=0}^{P} p_n(\mathbf{x},t)\Psi_n(\xi) \tag{6}$$

and performing the projection into each element of the polynomial basis leads to the following system of deterministic partial differential equations

$$\nabla \cdot \mathbf{u}_k = 0 \tag{7}$$

$$\frac{\partial \mathbf{u}_k}{\partial t} + \frac{1}{\|\Psi_k\|^2} \sum_{i=0}^{P} \sum_{j=0}^{P} e_{ijk} [\mathbf{u}_i \nabla] \cdot \mathbf{u}_j = -\frac{1}{\rho} \nabla p_k + \frac{1}{\|\Psi_k\|^2} \sum_{i=0}^{P} \sum_{j=0}^{P} e_{ijk} v_i \nabla^2 \mathbf{u}_j \tag{8}$$

where

$$e_{ijk} = \int_{\Omega} \Psi_i \Psi_j \Psi_k w(\xi) d\xi \tag{9}$$

and it was assumed that the viscosity may be a random variable (*r.v.*). The term e_{ijk} in equation (8) is a sparse, constant and symmetric tensor and can be calculated *a priori* with a high degree of accuracy. Equation (7) corresponds to the continuity equation and forms a set of independent partial differential equations, which means that all modes are divergence free. On the other hand, equations (8) form a coupled set. These equations are coupled by the convective term and the diffusive term. An important aspect of these equations is that they are "equivalent" for all the stochastic modes, which means that all modes are subjected to convection, diffusion and dissipation phenomena.

The solution of the system (7) and (8) provides the fields $\mathbf{u}_k(\mathbf{x},t)$ and $p_k(\mathbf{x},t)$ which contain all the statistics (statistical moments, correlations and PDF's) of the flow. Other quantities other than the primary variables will be calculated, such as the mean vorticity and mean energy. The mean vorticity (and its higher order modes) can be calculated easily because the rotational operator is linear, therefore

$$\omega = \nabla \times \vec{u} \qquad \Rightarrow \qquad \omega_k = \nabla \times \vec{u_k} \tag{10}$$

2.2 Numerical Method

A Runge-Kutta 4th order explicit time integration method together with sixth order spatial central differences approximation as used to solve the system of Navier-Stokes equations for the stochastic modes. This method consists in advancing the velocity fields

$$\mathbf{u}_k^* = \mathbf{u}_k^n + \Delta t \mathbf{F}(\mathbf{H}^n, \mathbf{H}^*) \tag{11}$$

The following equation is used to obtain the pressure correction

$$\frac{\mathbf{u}_k^{**} - \mathbf{u}_k^*}{\Delta t^*} = -\nabla p_k \tag{12}$$

The method has a computational cost for the solution of the coupled equations that is approximately $(P+1)$ times higher than the cost of solving the corresponding deterministic problem. The Laplacian operator in equation (12) was discretized using a second order central differences scheme in order to reduce the computational effort of solving $4(P+1)$ linear systems per time step. The parallelized Conjugate Gradient Method with optimized matrix/vector operations for this specific matrix was used. The sparseness of the e_{ijk} tensor was also taken into account in order to reduce the number of floating point operations.

The approximation error for the set of equations (5) and (6) has two sources, the truncation in the stochastic space and the second is the numerical discretization error. If we consider ε_P^2 to be the variance error of a random process $a(x,t,\xi)$ represented by its expansion coefficients $a_k(x,t)$, then

$$
\begin{aligned}
\varepsilon_P^2 &= \left| \sum_{k=1}^{\infty} a_k^2(x,t)\|\Psi_k\|^2 - \sum_{k=1}^{P} \tilde{a}_k^2(x,t)\|\Psi_k\|^2 + \varepsilon_{\Delta x} \right| \\
&= \left| \underbrace{\sum_{k=1}^{P} (a_k^2(x,t) - \tilde{a}_k^2(x,t))\|\Psi_k\|^2}_{I} + \underbrace{\sum_{k=P+1}^{\infty} a_k^2(x,t)\|\Psi_k\|^2}_{II} + \underbrace{\varepsilon_{\Delta x}}_{III} \right|
\end{aligned}
\tag{13}
$$

In equation (13) the approximation error sources correspond to: term *I* is the error due to the finite mode approximation where the computed modes $\tilde{a}_k(x,t)$ are slightly different from the exact solution modes $a_k(x,t)$; term *II* is the error due to not considering stochastic modes higher than *P* and term *III* is the numerical discretization error. These terms are not independent and it can occur that the magnitude of the terms higher than *P* are small but the error term *I* is large due to the coupling of the equations. The coupled system of equations (8) and (9) were solved considering several approximations and the results obtained with $P = 7$ displayed negligible contribution to the higher order modes. This requires the solution of 8 systems of momentum and continuity equations comprising 24 strongly coupled differential equations in a numerical mesh comprising $O[10^5]$ points. The instantaneous random velocity and pressure fields are obtained through the calculation of the coefficients in these equations. The first mode in the expansions (5) and (6) corresponds to the mean velocity and pressure, respectively.
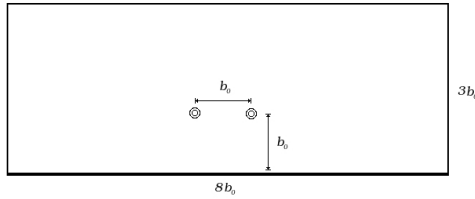

Figure 1: Computational domain and initial setup.

3   Results

3.1   *Deterministic evolution of a vortex pair in ground effect*

The computational domain used ($[-4,4] \times [0,3]$) is represented in Figure 1 with the vortices core size being $r_0 = 0.05b_0$. An algebraic vortex model was considered and the Reynolds number defined in terms of the initial circulation is equal to $Re = \Gamma_0/\nu = 5000$. The algebraic model is defined by equations (14), (15) and (16) for the vorticity, circulation and tangential velocity, respectively.

$$\omega(r) = \frac{\Gamma_0}{\pi} \frac{r_0^2}{(r^2 + r_0^2)^2} \qquad (14)$$

$$\Gamma(r) = \Gamma_0 \frac{r^2}{r^2 + r_0^2} \qquad (15)$$

$$v_\theta(r) = \frac{\Gamma(r)}{2\pi r} = \frac{\Gamma_0}{2\pi} \frac{r}{r^2 + r_0^2} \qquad (16)$$

A numerical grid comprised 800×300 points and the Courant number was equal to 0.4. The grid spacing of $r_0/\Delta x = 5$ was found to be enough to obtain a good numerical representation of the solutions. The boundary conditions correspond to first order extrapolation for the velocities at the open boundaries and no slip condition at the ground. Figure 2 shows the deterministic vorticity contour, for comparison purposes.

Initially, a favorable pressure gradient near the ground, due to the vortex induced velocity, causes the development of a boundary layer. When $t^* = 1$ the streamlines curvature is enough to impose an adverse pressure gradient to the boundary layer causing it to detach. This detached vortex filament rolls-up into a secondary vortex of opposite sign which induces the rebound of the primary vortex.

Duponcheel (2006) and Winckelmans (2006) showed that three-dimensional effects become important after the non-dimensional time $t^* = 3$. Their origin is caused by a short wave instability in the secondary vortex which is a purely three-dimensional effect caused by self induction. In this work the calculations will be made in the range of validity of the two-dimensional approximation, up to $t^* = 3.82$, corresponding to one loop of the secondary vortex.

3.2   *Stochastic Vortex Evolution in Ground Effect*

The statistics calculated a posteriori comprised: i) temporal evolution of the most probable trajectory and their error bar for a confidence interval of 90%, ii) temporal
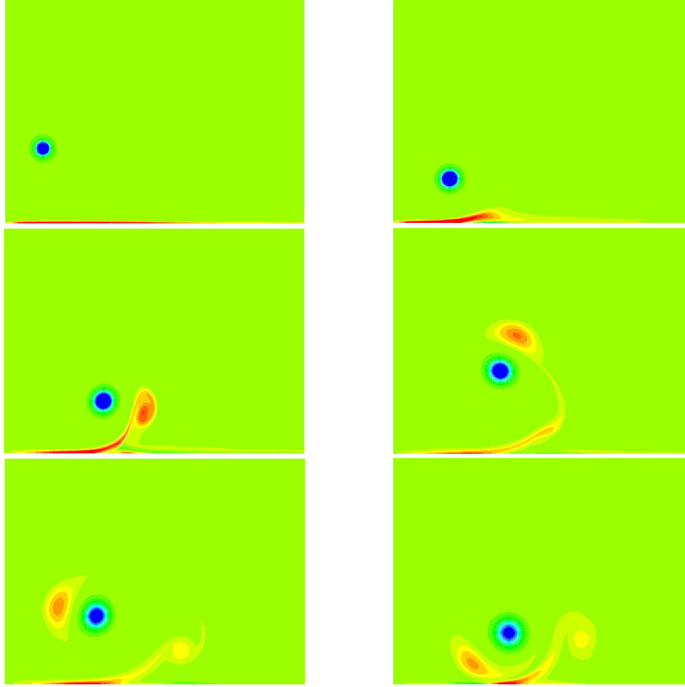
Figure 2: Deterministic wake vortices vorticity field evolution ($t^* = 0.00; 0.80; 1.59; 2.39; 3.18; 3.82$).

evolution of the mean energy and their error bar for a confidence interval of 90%, iii) Temporal evolution of a measure of circulation, expressed as Γ_{5-15} and its error bar for a confidence interval of 90%. The parameter Γ_{5-15} is a measure of the vortex strength and is used to enable comparison of circulation data of diverse investigations and is defined by equation (17).

$$\Gamma_{5-15} = \frac{1}{\frac{b}{6}} \int_{b/12}^{b/4} \Gamma(r) dr \qquad (17)$$

where b is the aircraft's wingspan which is related to the distance between the two wake vortices by $b_0/b = \pi/4$. The symbol Γ_{5-15} originally arise associated with $b = 60m$, see, e.g. Gerz (2005). The computation of Γ_{5-15} requires the integration of the local random circulation to obtain the mean value. The error, bar for a 90% confidence interval, establishes the range of variation for the Γ_{5-15} along the most probable trajectory. Numerical calculations will be presented for the temporal evolution of a vortex pair with parametric uncertainty either in the initial vortice
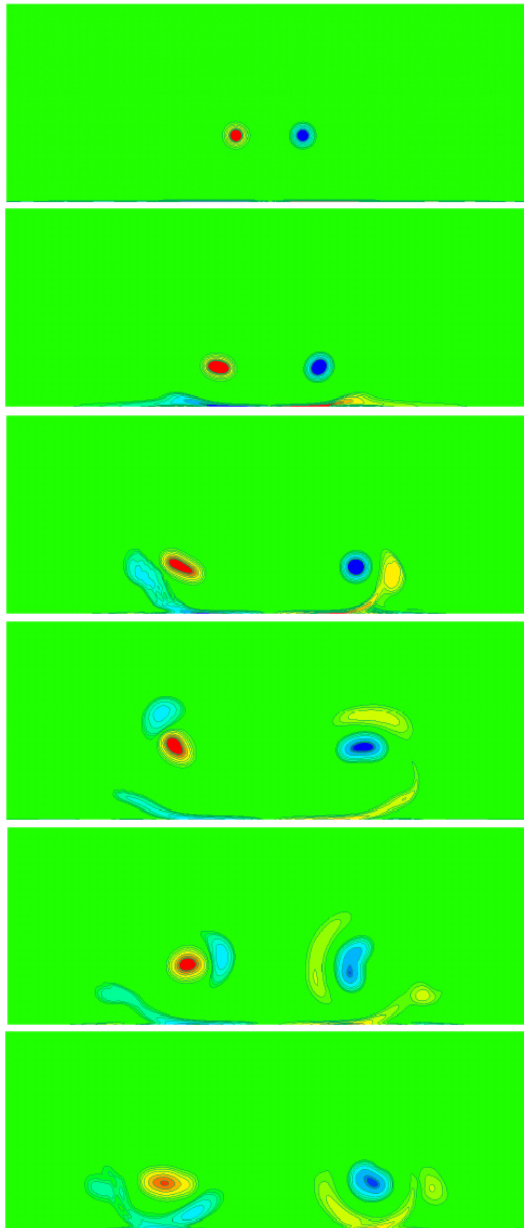
Figure 3: Symmetric wake vortices mean vorticity field evolution with random initial circulation with cv=10% ($t^* = 0.00; 0.80; 1.59; 2.39; 3.18; 3.82$).

location or their circulation, Reynolds number, $Re = \Gamma_0/\nu$. The uncertainty is characterized by a constant probability of occurrence, Beta probability, and a variability of 10%. One should mention that mean variables correspond to the ensemble average of a large number of events (each corresponding to a vortex evolution from a certain value with the initial uncertainty range considered). The relation between the mean velocity field and the mean vorticity field is linear with respect to the expansion, therefore the mean vorticity can be obtained from those fields. Although the ensemble vorticity is not a physical quantity, it contains information from all possible solutions and gives indication of the most probable set of outcomes. The point of maximum vorticity (or local vorticity centroid) is related to the location were it is most probable to find a given vortex. Consequently the mean trajectory is defined by these points (details are presented in appendix A).

3.2.1   Random Initial Circulation

An Uniform (Beta) initial circulation, $\Gamma(\xi) = \Gamma_0 + \Gamma_1(\xi)$ where ξ $U(-1,1)$ was considered for a coefficient of variation cv of 10%, for the left vortex (vortex 1), (standard deviation divided by the mean value, $cv^2 = V[\xi]/E[\xi]^2$). The initial condition for each mode is obtained by applying the definition of expected value and variance to $\Gamma(\xi)$. After this procedure, a relation between the coefficients and the desired mean and variance for the circulation is obtained.

An approximation with $P = 6$ is sufficient to capture the most important features of the high order statistics and provides very good estimates for the mean variables. Tests with very low uncertainty input, $cv = 1\%$ lead to results that are close to the deterministic denoting numerical consistency with the deterministic Navier-Stokes equations.

Figure 3 shows isocontours of the ensemble averaged vorticity at different instants obtained with the left vortex initial circulation with a coefficient of variation equal to 10%. It is worth mention that the ensemble averaged vorticity, like it would result from tens of thousands of $2D$ solutions (samples) with different initial circulations has no direct physical meaning.

Initially the ensemble average vortices have a circular shape as in the deterministic case, but as they approach the ground they become slightly of elliptic shape because of the dispersion of the trajectories. The left vortex, has an initial random circulation, and induces a random descendent velocity field to the right vortex affecting its trajectory. The random circulation of the left vortex produces a loss of symmetry and has an important effect on the other vortex. For this level of variability of the random input the ensemble mean vortices still maintain their structure after statistical averaging. The left vortex seems to depend essentially in the transport and diffusion of its own initial randomness. An analysis of the ensemble average

vorticity field shows that the right vortex variability is related to non-local effects, the induced random velocities, which act as an uncertainty source that affects the vortex trajectory and shape. The variability increases with time due to the loss of correlation caused by the dispersion of the possible trajectories.
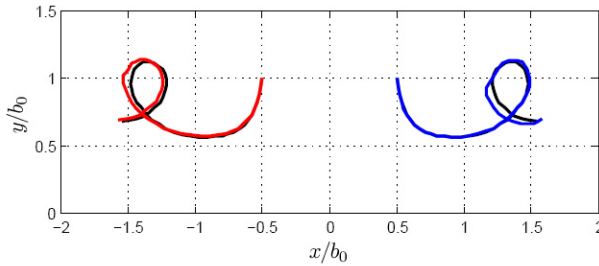

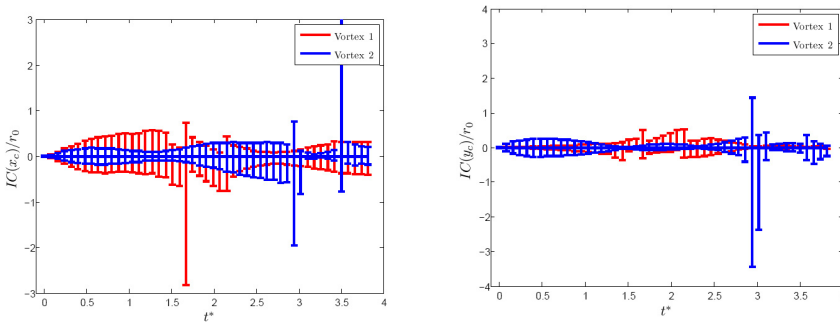Figure 4: Vortices most probable trajectory (Random initial circulation test case).

Figure 5: Vortices position error bar for a confidence interval of 90% (Random initial circulation test case), a) longitudinal coordinate, b) normal coordinate

Figure 5a) and b) show the error bars for the coordinates of the most probable vortex centroids $IC(x_c)/r_0$, and $IC(y_c)/r_0$, for a 90% interval of confidence. The error bar of the vortices trajectory is directly affected by the circulation 10% uncertainty and is a measure of the variability along the most probable trajectory (figure 4) and is calculated by considering the vortex position as the vorticity centroid. Furthermore, this centroid is considered as a random variable and therefore can be represented in terms of the polynomial chaos expansion (see the Appendix for details). The obtained expansion for a vortex centroid is used to calculate the r.v.'s probabil-
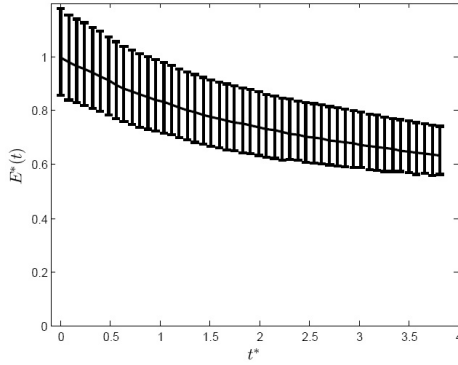
Figure 6: Mean energy decay and its error bar (Random initial circulation test case).
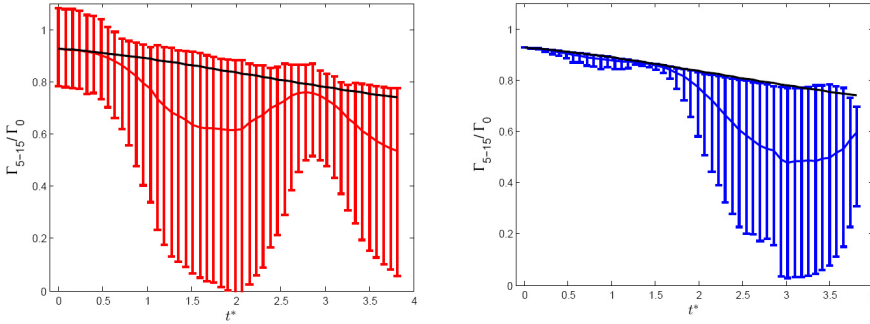

Figure 7: Circulation parameter for each vortex (Random initial circulation test case).

ity density function. The error bar for a 90% confidence interval is calculated by integrating the obtained PDF at a given time and position of the vortex.

Figure 5a) shows the error bars for the longitudinal coordinate of the vortex locations, due 10% variability of initial circulation and results in a region within the $2r_0$ range for a 90% confidence interval along the most probable trajectory. The normal coordinate as a small error bar, less than r_0. The temporal evolution of the energy's statistics is also obtained from the calculation of its polynomial chaos representation. This quantity has direct physical meaning regarding the average energy decay of a vortex pair (within the uncertainty considered for the initial circulation field). It is interesting to see that the mean energy decay (figure 6) remains almost unaffected by the random input, though having a large uncertainty associated to it. Clearly at $t^* = 0$ the error bar denotes the considered uncertainty in circulation and

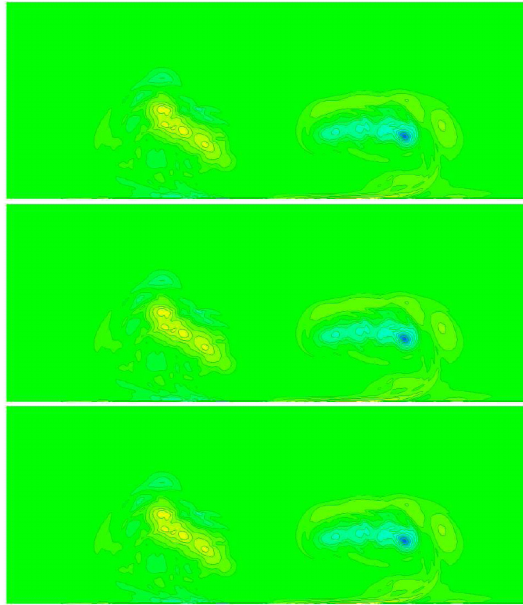there is a slight decrease of the error bar with time evolution.

Figure 8: Mean vorticity field evolution for $cv = 20\%$ ($t^* = 0.80; 1.59; 2.39$). Random initial circulation test case.
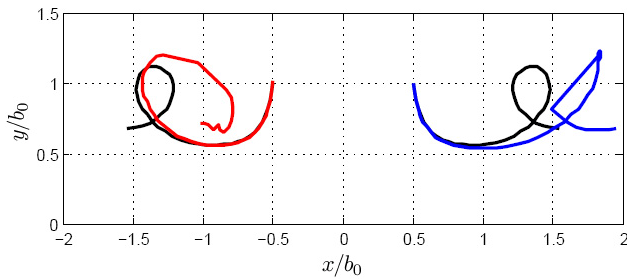

Figure 9: Deterministic and most probable (mean) trajectory (Random initial position test case).

Figure 7 shows the Γ_{5-15}/Γ_0 confidence interval as a function of time. The straight line indicates the deterministic evolution of the circulation that is a physical quantity of prime interest. The ensemble averaged Γ_{5-15} value given by the curve line has no physical sense and is kept to give a comparison with the deterministic case.
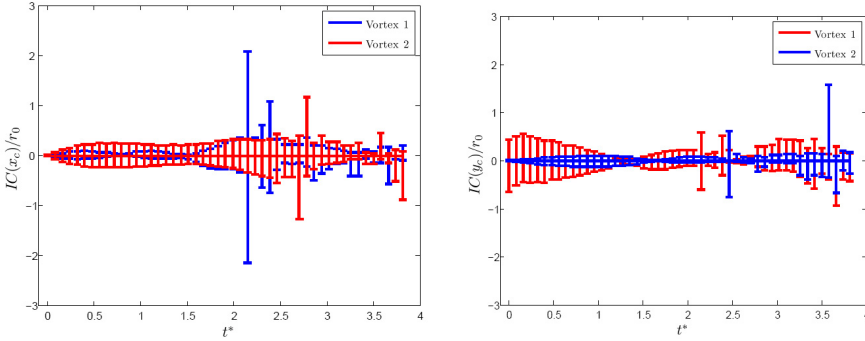
Figure 10: Vortices position confidence interval (Random initial position test case)., a) longitudinal coordinate, b) normal coordinate.
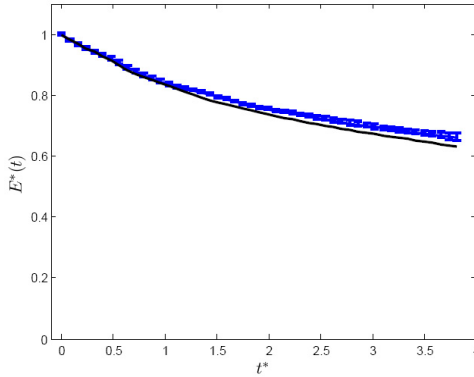

Figure 11: Energy decay (Random initial position test case).

The value of Γ_{5-15} is obtained from the integration of the vorticity field in a circle centered in the most probable vortex trajectory position (vortex core position). Consequently, for a high dispersion of the vortex trajectories the Γ_{5-15} error bar value may be very high. The initial random circulation of one of the vortices presents values that may be 10% higher than the mean value, it explains why there are higher Γ_{5-15} values than the deterministic case, meaning that there are vortices with a higher initial circulation that closely follow the most probable trajectory.

Figure 7a) shows the Γ_{5-15}/Γ_0 error bar corresponding to the vortice with the 10% variability. For $1.25 \leq t^* \leq 2.5$ the interaction of the main vortex with the created secondary vortex originating a large uncertainty and the possible vortex trajectories
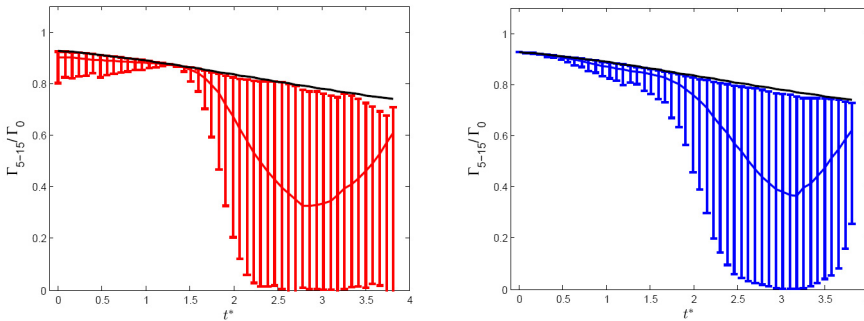
Figure 12: Circulation parameter for each vortex (Random initial position test case).

are different from the most probable one, originating a large error bar. Figure 7b) shows that up to $t^* = 2$ the circulation error bar remains close to the deterministic and afterwards a large error bar appears due to dispersion of vortex trajectories as a consequence of the events inherent to the dispersion of trajectories.

The level of variability of the random input chosen ($cv = 10\%$) was sufficiently low to allow a relative small number of approximation modes. Random inputs of $cv = 20\%$, not shown for conciseness were also tested and the results showed that, due to averaging, the mean solution will break down into smaller structures consisting of ensemble averaged vorticity peaks. In this case it is not possible, after the rebound ($t^* = 1.0$), to find singular ensemble averaged "coherent vortices". The ensemble of possible solutions (events) will form large clouds consisting in various peaks of vorticity related to clustered groups of events. In this case high order statistics, i.e. events far from the mean solution, will play an important role and approximations with $P >> 7$ will be required but for this level of randomness it will be very difficult to extract the most probable vortex paths.

3.2.2 *Random Initial Position*

A uniformly distributed random vortex position, in the vertical coordinate, was considered ($y(\xi) = y_0 + y_1 \xi$) with a 10% coefficient of variation. The initial random condition was represented in terms of the stochastic modes, i.e., it was necessary to have a spectral representation of the initial fields representing a vortex randomly positioned vortex. The discrete least squares method was used to obtain the coefficients of the expansion. The velocity field $U[u(x,y), v(x,y)]$ which defines the vortex can be subjected to a random input through $y(\xi)$. This is done simply by substituting this r.v. in the defining equations (14), (15) and (16). The difficulty

here is that one needs to generate the stochastic modes U_k which will form the initial condition for the system of equations (7) and (8). In some cases the analytic integration of the expressions may not be possible and in other cases an accurate numerical integration approach may become difficult to obtain. This was solved by approximating the fields using a least squares approach where the basis functions were chosen to be the orthogonal polynomials. The least squares problem solution yields the stochastic modes directly. Furthermore, if the collocation points are the zeros of the orthogonal polynomials, then the least squares matrix will have good numerical properties. The collocation points chosen were the zeros of the first 10 Jacobi polynomials (defined in the interval $[-1, 1]$) and the points $\{-1, 1\}$, which gives a total of 53 collocation points.

For $t^* = 0$ the ensemble averaged vortex shows an elliptic shape as the result of the averaging operation of a set of randomly sampled fields consisting in vortices at different locations along the vertical position. An approximation of $P = 7$ is sufficient for the representation of this initial condition because the relation of the first and the seventh mode magnitudes is of $O[10^{-2}]$. Both the mean solution and their variance display negligible representation errors. In this case, the circulation is the same for both vortices and the left ensemble mean vortex of initial elliptic shape becomes of circular shape until it reaches the rebound height. This means that the variability will initially decrease. After the rebound, the set of possible paths increases rapidly due to the interaction with the secondary vortex which causes the ensemble mean vortex to regain its elliptical shape.

The vortices trajectories are quite different from the deterministic and they present jumps and oscillations because the ensemble averaged vorticity structures displays multiple peaks of vorticity corresponding to clustered subsets of solutions, which explain the irregularity of the trajectories. The variability in the vortices trajectories is characterized by an amplitude of the confidence interval of length approximately of $2r_0$ (figure 8). The mean energy, presented in figure 9 decays slower than the deterministic case. Its uncertainty is much smaller than in the previous case of the uncertainty in the circulation. As in the previous case a large variability in the Γ_{5-15}/Γ_0 circulation parameter was found, see figure 10 for the time instants where the main vortex interacts with the secondary vortex.

4 Conclusion

The evolution of a vortex pair in ground effect and under various random inputs was investigated using the full $2D$ incompressible Navier-Stokes equations and the Polynomial Chaos Expansion method for the representation of stochastic processes. Two uncertainty sources have been considered: i) Initial circulation of one of the vortices and ii) Initial position of one of the vortices. A variability of the random

input of 10% was considered with a uniform probability of occurrence for each of the random variables. In general, approximations of $P = 6$ or $P = 7$ were sufficient to capture the most important features of the randomness propagated by the stochastic Navier-Stokes equations despite of the continuous loss of correlation in time that is caused by the increase of the higher order statistics (statistical moments) importance. For the low variability with 10% initial uncertainty considered and up to $t^* = 3$ the following conclusions can be withdrawn:

i)The non-linearity of the propagation of the uncertainty from the initial circulation or vortex position is amplified with the vortex interaction with the secondary vortex. This is notorious in the Γ_{5-15} and for some cases in the error bar of the vortices most probable trajectories, which are of $\pm r_0$.

ii)The energy decay evolution depends on the cases considered. For the case of uncertainty in the circulation the ensemble average energy was indistinguishable from the deterministic result. For the uncertainty in the vortex position the energy decayed is slower than the deterministic evolution.

iii)A fast decay of the mean Γ_{5-15} means that the probability is high to find events outside the Γ_{5-15}/Γ_0 integration range surrounding the most probable vortex trajectory.

iv)The number of stochastic modes and the numerical resolution considered allowed to obtain highly accurate solutions for the $2D$ unsteady flow. For higher variability coefficients, e.g. $cv = 20\%$, the produced strong amplification of the uncertainty input would require $P >> 7$ and the formation of sets of clustered (similar) discrete clouds of random events, displayed in the ensemble averaged vorticity, denote a high dispersion of the vortex trajectories making the most probable vortex position difficult to calculate. The destruction of the ensemble averaged vortices coherence means that large a dispersion of trajectories occurred.

v) The computational cost of solving a system of $P + 1$ sets of Navier-Stokes like equations was around 9 times higher than the deterministic case corresponding to a high computational demand regarding a $2D$ flow case , nevertheless, it is orders of magnitude smaller than the estimated Monte Carlo based simulation.

References

Caduci, D. (2003):   *Sensitivity and Uncertainty ANALYSIS : Theory, vol I.* Chapmann & Hall/CRC.

Cameron, R.; Martin, W. (1947): The orthogonal development of non-linear functionals in series of fourier-hermite functionals. *Ann. of Math.*, vol. 48, no. 2, pp. 385–392.

Cui, T., L. W.; Yu, D. (2009): Topological Approach for Analysing and Modelling the Aerodynamic hysteresis of an Airfoil. *CMES-Computer Modelling in Engineering & Sciences*, vol. 45, pp. 273–293.

Duponcheel, M., L. T. B.-L. W. G. (2006): Simulation of three-dimensional wake vortices in ground effect using a fourth order incompressible code. *In 7th Congress on Theoretical and Applied Mechanics. Mons, Belgium.*, vol. 229.

Fleissner, F., H. T. H.-M.; Eberhard, P. (2009): Uncertainty Analysis for a Particle Model of Granular Chute Flow. *CMES-Computer Modelling in Engineering & Sciences*, vol. 52, pp. 181–196.

Gao, W., S. C. T.-L. F. (2009): Probabilistic Interval Response and Reliability Analysis of Structures with a Mixture of Random and interval Properties. *CMES-Computer Modelling in Engineering & Sciences*, vol. 46, pp. 151–189.

Gerz, T., H. F. B.-W. K. F. T. A. W. G. (2005): Research towards a wake-vortex advisory system for optimal aircraft spacing. *Comptes Rendus Physique*, vol. 6, pp. 501–523.

Ghanem, R.; Spanos, P. (1991): *Stochastic Finite Elements: A Spectral Approach*. Springer-Verlag.

Knio, O.M., L. M. O. (2006): Uncertainty propagation in cfd using polynomial chaos decomposition. *Journal of Fluid Dynamics Research*, vol. 38, pp. 616–640.

Le Maître, O.; Najm, H.N., G. R.; Knio, O. (2004): Multi-resolution analysis of wiener-type uncertainty propagation schemes. *Journal of Computational Physics*, vol. 197, pp. 502–531.

Loeven, G.; Bijl, H. (2008): Probabilistic Collocation used in a two-STEP approach for uncertainty quantification in computational fluid dynamics. *CMES-Computer Modelling in Engineering & Sciences*, vol. 36, pp. 193–212.

Maître, O.P., K. O. N.-H. G. R. (2001): A stochastic projection method for fluid flow. basic formulation. *Journal Of Computational Physics*, vol. 173, pp. 481–511.

Najm, O. (2009): Uncertainty quantification and polynomial chaos techniques in computational fluid dynamics. *Annual Review of Fluid Mechanics*, vol. 41, pp. 35–52.

Parussini, L.; Pediroda, V. (2007): Fictitious domain with least-squares spectral element method to explore geometric uncertainties by non-intrusive polynomial

chaos method. *CMES-Computer Modelling in Engineering & Sciences*, vol. 22, pp. 41–46.

Parussini, L.; Pediroda, V. (2008):   Investigation of multi geometric uncertainties by different Polynomial Chaos methodologies using a fictitious domain solver. *CMES-Computer Modelling in Engineering & Sciences*, vol. 23, pp. 29–51.

Soize, C.; Ghanem, R. (2004):   Physical systems with random uncertainties: chaos representation with arbitrary probability measure. *SIAM, Journal on Scientific Computing*, vol. 26, no. 2, pp. 395–410.

Spalart, P. (1998): Airplane trailing vortices. *Annual Reviews of Fluid Mechanics*, vol. 30, pp. 107–138.

Turrin, S., H. M. S.-A. (2009): An Approach to Uncertainty Analysis of Rockfall Simulation. *CMES-Computer Modelling in Engineering & Sciences*, vol. 52, pp. 237–258.

Wiener, N. (1938):   The homogeneous chaos. *Amer. J. Math.*, vol. 60, pp. 897–936.

Winckelmans, G., C. R. D.-L. C. R. B. L. D. G. L. T. D. M. D. O. G. L. (2006): Direct numerical simulation and large eddy simulation of wake vortices: Going from laboratory conditions to flight conditions. *Proc. European Conference on Computational Fluid Dynamics, ECCOMAS CFD, Special Technology Session on Wake Vortex Research in Europe, Egmond aan Zee, The Netherlands.*

Xiu, D.; Karniadakis, G. (2002):   The wiener-askey polynomial chaos for stochastic differential equations. *SIAM, Journal on Scientific Computing*, vol. 24, no. 2, pp. 619–644.

Appendix A: Determination of the vortices location and statistics

The vortices location at a given instant will be calculated in terms of two different definitions. The first was considered because it enables us to compare the results obtained with previously published results. This definition considers that the vortex is located at the point of maximum vorticity, i.e.

$$(x_c, y_c) = \max_{x,y \in A} |\omega(x,y)|$$

and provides a simple implementation. This definition is not suitable to evaluate the trajectories uncertainty, which leads us to the second definition. The vortex position can be defined has the centroid of the vorticity evaluated in some closed domain $B \subset A$

$$(\bar{x}, \bar{y}) = \frac{\int_B (x, y) |\omega(x, y)| ds}{\int_B |\omega(x, y)| ds}$$

A circular region centered at the point of maximum vorticity was considered to perform the integration. The vortex centroid depends on the shape of the vortex and, in general, is not coincident with the point of maximum vorticity (they are equal if the vortex has a circular shape, or more generally, if the vortex is bi-symmetrical). Therefore, the radius of the circular region was chosen such that the trajectories calculated with the two measures of the vortex position were approximately the same. After some numerical experimentation, a radius of $r'/r_0 = 6/5$ was chosen. Considering the centroid to a function of the basic random variable $\bar{x} = \bar{x}(\xi)$ and rewriting the previous as[1]

$$\bar{x}(\xi) \int_B \omega(x, y, \xi) ds = \int_B x \omega(x, y, \xi) ds$$

multiplying both sides of the equation by $\Psi_k(\xi)$ and integrating

$$\int_\Omega \left(\bar{x}(\xi) \int_B \omega(x, y, \xi) ds \right) \Psi_k(\xi) w(\xi) d\xi = \int_\Omega \left(\int_B x \omega(x, y, \xi) ds \right) \Psi_k(\xi) w(\xi) d\xi$$

Considering the left hand side of the equation[2]

$$\int_\Omega \left(\bar{x}_c(\xi) \int_B \omega(x, y, \xi) ds \right) \Psi_k(\xi) w(\xi) d\xi =$$

$$= \int_\Omega \left(\sum_{i=0}^P \bar{x}_i \Psi_i(\xi) \int_B \sum_j^P \omega_j(x, y) \Psi_j(\xi) ds \right) \Psi_k(\xi) w(\xi) d\xi$$

$$= \int_B \left(\int_\Omega \sum_{i=0}^P \sum_{j=0}^P \bar{x}_i \omega_j(x, y) \Psi_i(\xi) \Psi_j(\xi) \Psi_k(\xi) w(\xi) d\xi \right) ds$$

$$= \int_B \left(\sum_{i=0}^P \sum_{j=0}^P e_{ijk} \bar{x}_i \omega_j(x, y) \right) ds$$

Considering now the right hand side of the equation

---

[1] The modules were dropped to simplify the notation.
[2] The integrals can be interchanged and $\bar{x}$ is not a function of the spacial variables

$$\int_{\Omega} \left(\int_B x\omega(x,y,\xi)ds \right) \Psi_k(\xi)w(\xi)d\xi =$$

$$= \int_B \left(\int_{\Omega} x\sum_{i=0}^{P} \omega_i(x,y)\Psi_i(\xi)\Psi_k(\xi)w(\xi)d\xi \right) ds$$

$$= \|\Psi_k\|^2 \int_B x\omega_k(x,y)ds$$

To obtain the $(P+1)$ coefficients of the centroids expansion one must solve the linear system

$$\int_B \left(\sum_{i=0}^{P}\sum_{j=0}^{P} e_{ijk}\bar{x}_i\omega_j(x,y) \right) ds = \|\Psi_k\|^2 \int_B x\omega_k(x,y)ds$$